Histochem Cell Biol (2007) 127:273–290
DOI 10.1007/s00418-006-0254-6

ORIGINAL PAPER

Localization of the pre-squalene segment of the isoprenoid biosynthetic pathway in mammalian peroxisomes

Werner J. Kovacs · Khanichi N. Tape · Janis E. Shackelford · Xueying Duan · Takhar Kasumov · Joanne K. Kelleher · Henri Brunengraber · Skaidrite K. Krisans

Accepted: 31 October 2006 / Published online: 19 December 2006

Abstract Previous studies have indicated that the early steps in the isoprenoid/cholesterol biosynthetic pathway occur in peroxisomes. However, the role of peroxisomes in cholesterol biosynthesis has recently been questioned in several reports concluding that three of the peroxisomal cholesterol biosynthetic enzymes, namely mevalonate kinase, phosphomevalonate kinase, and mevalonate diphosphate decarboxylase, do not localize to peroxisomes in human cells even though they contain consensus peroxisomal targeting signals. We re-investigated the subcellular localization of the cholesterol biosynthetic enzymes of the pre-squalene segment in human cells by using new stable isotopic techniques and data computations with isotopomer spectral analysis, in combination with immunofluorescence and cell permeabilization techniques. Our present findings clearly show and confirm previous studies that the pre-squalene segment of the cholesterol biosynthetic pathway is localized to peroxisomes. In addition, our data are consistent with the hypothesis that acetyl-CoA derived from peroxisomal β-oxidation of very long-chain fatty acids and medium-chain dicarboxylic acids is preferentially channeled to cholesterol synthesis inside the peroxisomes without mixing with the cytosolic acetyl-CoA pool.

Keywords Cholesterol biosynthesis · Isoprenoid · Peroxisomes · Mass isotopomer distribution · HepG2

Abbreviations

AOX	Acyl-CoA oxidase
FPP	Farnesyl diphosphate
GFP	Green fluorescent protein
HMGCR	HMG-CoA reductase
IDI1	Isopentenyl diphosphate isomerase 1
ISA	Isotopomer spectral analysis
MID	Mass isotopomer distributions
MPD	Mevalonate diphosphate decarboxylase
MVK	Mevalonate kinase
PEX	Peroxin
PMP	Peroxisomal membrane protein
PMVK	Phosphomevalonate kinase
PP	Diphosphate
PTS	Peroxisomal targeting signal

W. J. Kovacs · K. N. Tape · J. E. Shackelford · S. K. Krisans
Department of Biology, San Diego State University,
San Diego, CA, USA

W. J. Kovacs
Department of Anatomy and Cell Biology,
Division of Medical Cell Biology,
Justus Liebig University of Giessen,
Aulweg 123, 35385 Giessen, Germany
e-mail: werner.kovacs@anatomie.med.uni-giessen.de

X. Duan · T. Kasumov · H. Brunengraber
Department of Nutrition,
Case Western Reserve University, Cleveland, OH, USA

J. K. Kelleher
Department of Biomedical Engineering,
Massachusetts Institute of Technology,
Cambridge, MA, USA

W. J. Kovacs (✉)
Institute of Cell Biology, Schafmattstrasse 18,
ETH-Hönggerberg, HPM, F 39.2, 8093 Zürich, Switzerland
e-mail: werner.kovacs@cell.biol.ethz.ch

Introduction

Peroxisomes are ubiquitous and highly versatile organelles of eukaryotic cells whose enzymes participate in various metabolic pathways including: (1) β-oxidation

of a specific set of lipids which cannot be processed by mitochondria (very long-chain fatty acids, long-chain dicarboxylic acids, eicosanoids, and bile acid intermediates), (2) biosynthesis of cholesterol, isoprenoids, and ether-phospholipids (plasmalogens), and (3) reactive oxygen species metabolism (Mannaerts et al. 2000; Wanders 2004; Kovacs et al. 2002; Schrader and Fahimi 2004). Two *p*eroxisomal *t*argeting *s*ignals (PTSs), PTS1 and PTS2, account for the transport of most enzymes involved in these metabolic pathways into the peroxisome matrix (Subramani 1993). PTS1, the major targeting signal, is a carboxyl-terminal tripeptide with the consensus sequence (S/C/A)(K/R/H)(L/M) and targets proteins to the peroxisome in all eukaryotic organisms examined, from yeast to man. PTS1-dependent transport is mediated by a shuttling receptor, the peroxin Pex5p, which recognizes the PTS1 tripeptide in the cytoplasm and mediates the import of PTS1-containing proteins into the peroxisome (Dammai and Subramani 2001). Recent analysis of sequence variability in the PTS1 motif revealed that, in addition to the known C-terminal tripeptide, at least nine residues directly upstream are important for signal recognition in the PTS1-Pex5p receptor complex (Neuberger et al. 2003a). The importance of specific residues near the C-terminus appears to be particularly important if the C-terminal tripeptide deviates from the conservative consensus PTS1 (Lametschwandtner et al. 1998). A small subset of peroxisomal matrix proteins is targeted by PTS2, which consists of a degenerate nine-residue signal located internally or near the amino terminus. The consensus PTS2 has the sequence—(R/K)(L/V/I)X5(H/Q)(L/A)—(Rachubinski and Subramani 1995). Some PTS2 proteins have the PTS2 removed by a peroxisomal peptidase upon entering the peroxisomal lumen (Subramani 1993). The import of PTS2 proteins into peroxisomes is mediated by the hydrophilic cytoplasmic receptor Pex7p, which is also dependent on the long isoform of Pex5p (Mukai et al. 2002; Ghys et al. 2002).

Isoprenoids and isoprenoid compounds play vital roles in all living systems, e.g. in the structure of cells, in electron transport, in glycoprotein synthesis, in cell to cell signaling, in transfer RNAs, in the structure of organisms, and in the interactions between organisms (Goldstein and Brown 1990). The enzymes that produce cholesterol and other isoprenoids are distributed in different subcellular compartments (Kovacs et al. 2002). The prevailing view has been that cholesterol biosynthetic reactions occur in the cytoplasm and endoplasmic reticulum (ER). However, numerous studies have indicated that the early steps in the isoprenoid/cholesterol biosynthetic pathway occur in peroxisomes (Keller et al. 1985, 1986; Stamellos et al. 1992; Biardi et al. 1994; Krisans et al. 1994; Biardi and Krisans 1996; Chambliss et al. 1996; Paton et al. 1997; Olivier et al. 1999, 2000; Gupta et al. 1999; Kovacs et al. 2001). In addition, with the exception of 3-hydroxy-3-methylglutaryl-coenzyme A (HMG-CoA) reductase, the enzymes contain functional PTSs (Table 1). Furthermore, the enzymes catalyzing the conversion of mevalonate to farnesyl diphosphate (FPP) appear to be exclusively peroxisomal. Due to these facts, a new model for the compartmentation of the cholesterol biosynthetic pathway has been presented (Kovacs et al. 2002).

However, the role of peroxisomes in cholesterol biosynthesis has recently been questioned in several reports concluding that three of the peroxisomal cholesterol biosynthetic enzymes, namely mevalonate kinase (MVK), phosphomevalonate kinase (PMVK), and mevalonate diphosphate decarboxylase (MPD), do not localize to peroxisomes in human cells even though they contain consensus PTSs (Hogenboom et al. 2004a, b, c).

Since the data from Hogenboom et al. (2004a, b, c) are conflicting with the concept of a peroxisomal segment of cholesterol biosynthesis and our previous work was done mainly using rat liver and Chinese hamster ovary (CHO) cells, we decided to re-investigate the subcellular localization of the "pre-squalene" cholesterol biosynthetic enzymes in human cells. By using new stable isotopic techniques and data computations with isotopomer spectral analysis (ISA), in combination with immunofluorescence and selective permeabilization techniques, we clearly confirm our previous studies obtained in rats and CHO cells. In addition, we provide new evidence compatible with the presence of the pre-squalene part of sterol synthesis in peroxisomes. Furthermore, we show that acetyl-CoA derived from peroxisomal β-oxidation of very long-chain fatty acids and medium-chain dicarboxylic acids is preferentially channeled to cholesterol synthesis inside the peroxisomes without mixing with the cytoplasmic acetyl-CoA pool.

Materials and methods

Antibodies

The following antibodies against cholesterol biosynthetic enzymes were used: rabbit polyclonal anti-(HMG-CoA) reductase (a gift of P. Edwards, University of California at Los Angeles), anti-MVK (Biardi et al. 1994), anti-(isopentenyl diphosphate dimethylallyl diphosphate) (IPP) isomerase 1 (Paton et al. 1997; Kovacs et al. 2004a), and anti-FPP synthase (Krisans

et al. 1994); mouse monoclonal anti-(HMG-CoA) reductase (a gift of M.S. Brown and J.L. Goldstein, University of Texas Southwestern Medical Center, USA). Antibodies against the following intracellular compartments were used: (1) Peroxisomes: rabbit polyclonal anti-guinea pig catalase, anti-rat acyl-CoA oxidase (AOX) and anti-rat PMP70 (peroxisomal membrane protein 70) (Beier et al. 1988; Lüers et al. 1993) (a gift of A. Völkl, University of Heidelberg); sheep polyclonal anti-human catalase (The Binding Site, Birmingham, UK); (2) mitochondria: rabbit polyclonal anti-cytochrome *c* (Santa Cruz Biotechnology, Santa Cruz, CA); (3) lysosomes and endosomes: mouse monoclonal anti-human Limp-1 (CD63), anti-Rab5 and anti-(early endosome antigen 1) (EEA1) (BD Biosciences-Pharmingen, San Diego, CA); mouse monoclonal anti-human Lamp-2 (lysosomal associated membrane protein-2) (Research Diagnostics, Flanders, NJ). The monoclonal mouse antibody against the *myc* epitope was obtained from Invitrogen (Carlsbad, CA, USA). Species-specific anti-IgG antibodies conjugated to Alexa 488 (A-11008, A-11001), 594 (A-11012, A-11005), and 647 (A-21244, A-21235) were obtained from Molecular Probes (Eugene, OR, USA). The Texas Red dye-conjugated donkey anti-sheep IgG (#713-075-147) was obtained from Jackson ImmunoResearch (West Grove, PA, USA).

Cell culture

HepG2 cells (Aden et al. 1979), derived from a human hepatoblastoma, were obtained from the American Tissue Culture Collections (Rockville, MD) and grown in Dulbecco's Modified Eagle Medium:Ham's F-12 (1:1, v/v) medium supplemented with 10% (v/v) fetal calf serum (FCS). The CHO cell line, CHO-K1, and the peroxisome-deficient mutant CHO lines (ZR-78, ZR-82, and ZR-87), which are all deficient in Pex2p, were obtained from Dr. Raphael A. Zoeller (Boston University School of Medicine, Boston, MA) and grown in Ham's F-12 medium supplemented with 10% (v/v) fetal calf serum. PEX2-transfected CHO-K1/pPEX2, ZR-78/pPEX2, ZR-82/pPEX2 and ZR-87/pPEX2 cells were maintained in the same medium containing 500 μg/ml G418. Cells were cultivated at 37°C in a humidified atmosphere of 5% CO_2 and 95% air. Cells were grown on collagenized coverslips in media containing 5% lipoprotein-deficient serum (Intracel, Frederick, MD) for 24 h prior to immunofluorescence studies using antibodies against endogenous cholesterol

Table 1 Sequences of functional PTS motifs in cholesterol biosynthetic enzymes

Protein name	Sequence of carboxy terminus including PTS1 motif	Organism	Accession number
Acetoacetyl-CoA thiolase	GGGASAMLI*QKL*	*Hs*	D90228
	GGGASALLI*EKL*	*Mm*	BC024763
	GGGASAVLI*EKL*	*Rn*	D13921
Phosphomevalonate kinase	LENLIEFIR*SRL*	*Hs*	BC007694
	LEHLLGFIQ*AKL*	*Mm*	AK003607
	NLLEFIH*AKL*QR	*Rn*	BC086349
Isopentenyl-PP isomerase	NQFVDHEKI*YRM*	*Hs*	AF271720
	SPFVDHEKI*HRL*	*Mm*	BC004801
	SPFVDHEKI*HRM*	*Rn*	AF003835
	PTS2 sequences		
HMG-CoA synthase	SVKTNLM*QL*	*Hs*	BC000297
	SVKSNLM*QL*	*Mm*	BC029693
	SVKSNLM*QL*	*Rn*	X52625
Mevalonate kinase	*KV*ILHGE*HA*	*Hs*	M88468
	*KV*ILHGE*HA*	*Mm*	BC005606
	*KV*ILHGE*HA*	*Rn*	M29472
Mevalonate-PP decarboxylase	*SV*TLHQD*QL*	*Hs*	U49260
	*SV*TLHQD*QL*	*Mm*	AJ309922
	*SV*TLHQD*QL*	*Rn*	U53706
Isopentenyl-PP isomerase	*HL*DKQQV*QL*	*Hs*	AF271720
	*HL*DEKQV*QL*	*Mm*	BC004801
	*NL*DEKQV*QL*	*Rn*	AF003835
Farnesyl-PP synthase	*NS*DVYA*QE*	*Hs*	J05262
	*KL*DAYN*QE*	*Mm*	BC048497
	*KL*DVHN*QE*	*Rn*	M34477
Consensus PTS1	(S/C/A)(K/R/H)(L/M)		
Consensus PTS2	(R/K)(L/V/I)X5(H/Q)(L/A)		

Hs *Homo sapiens*, Rn *Rattus norvegicus*, Mm *Mus musculus*

biosynthetic enzymes [HMG-CoA reductase (HMGCR), MVK, IDI1, and FPP synthase].

Vector construction

The construction of expression vectors for full-length acetoacetyl-CoA thiolase (ACAT1) containing a myc epitope tag between the mitochondrial and PTSs (Olivier et al. 2000), pEGFP-PMVK and pEGFP-PMVKΔPTS (Olivier et al. 1999) has been described before. The expression vector pDsRed2-Peroxi, which encodes a fusion of *Discosoma* sp. red fluorescent protein and the PTS1 "SKL", was purchased from Clontech. The vector expressing DsRed2 ending in QKL and EKL was generated by ligating the appropriate insert into the Not I and Pst I digested pDsRed2-Peroxi vector. The insert was generated using the primers 5′-caggactcctccctgcagga and 5′-cgcggccgctacagcttctgcttgta (for pDsRed2-QKL) and pDsRed2-Peroxi as the PCR template. PCR products were ligated into pCR4-TOPO vector (Invitrogen, Carlsbad, CA) and digested with Not I and Pst I. Subcloning and reading frame were verified by both restriction digest and DNA sequencing.

Transfection and immunofluorescence

Transient transfections were performed using the Lipofectamine 2000 reagent (Invitrogen, Carlsbad, CA) according to the manufacturer's instructions. Cells grown on collagen-coated glass coverslips were fixed with 4% paraformaldehyde in PBS, pH 7.4, permeabilized with 0.2% Triton X-100 and incubated with primary and secondary antibodies as described (Kovacs et al. 2004b).

Fixed cells labeled with antibodies and/or fluorescent proteins were optically sectioned into z-stacks, with the pinhole set to 1 Airy unit. Fluorescent dyes were imaged sequentially in frame interlace mode to eliminate cross-talk between the channels. Fluorescence was visualized using a DM-IRBE confocal microscope (Leica, Wetzlar, Germany) and images were processed using TCS-NT software (Leica). A representative optical section is presented for each data set.

Cell permeabilization with digitonin

Cell permeabilization experiments were performed as described by Biardi and Krisans (1996) with a few modifications. HepG2 cells were seeded at a density of 3.0×10^6 on 100-mm plates and grown to 50% confluence. The cells were washed with PBS and transferred to media containing 5% lipoprotein-deficient serum (Intracel, Frederick, MD) for 72 h prior to the experiment. On the day of the experiment, the cells were washed twice with ice-cold KH buffer (50 mM HEPES, 110 mM KOAc, pH 7.2), transferred to ice and incubated in KHM buffer (20 mM HEPES, 110 mM KOAc, 2 mM MgOAc, pH 7.2) containing various concentrations of digitonin (0, 20, 50, 150, 500, and 1,000 μg/ml). After 5 min, the buffer was collected as supernatant fractions and kept on ice. The cells were washed twice with ice-cold KH buffer and subsequently incubated in KH buffer containing 1,000 μg/ml digitonin for 30 min. These latter fractions were referred to as pellet fractions. The activities of phosphoglucose isomerase (PGI), a cytosolic marker enzyme, and catalase, a peroxisomal marker enzyme, were measured as described previously (Kovacs et al. 2001).

[^{13}C]Acetyl-CoA enrichment for sterol synthesis

[U-$^{13}C_{12}$]Dodecanedioic acid was obtained from Isotec (Miamisburg, OH). [1,2,3,4-$^{13}C_4$]Docosanoic acid was synthesized from stearyl bromide and [U-$^{13}C_4$]acetoacetate ethyl ester (Zhang et al. 1994). The purity of the synthesized compounds was verified by gas chromatography-mass spectrometry (GC-MS) and NMR.

Docosanoic acid was dissolved either in ethanol or in 2.8 mM NaOH containing 10% fatty acid-free bovine serum albumin (faf-BSA). Dodecanedioic acid was dissolved in 1 M NaOH and added to the media containing 5% lipoprotein-deficient serum. HepG2, CHO-K1, and peroxisome-deficient CHO cells were incubated with either 0.1 mM and 0.2 mM unlabeled and [1,2,3,4-$^{13}C_4$]docosanoate or 1, 2, and 3 mM unlabeled and [U-$^{13}C_{12}$]dodecanedioate for 24, 48, and 72 h. Media were changed every day. Cells were washed once with ice-cold PBS containing 2 mg/ml faf-BSA and twice with PBS prior to collection. Lipid extracts were saponified in KOH-ethanol before extraction of the sterols with petroleum ether. The aqueous phase was acidified, and fatty acids were extracted with petroleum ether. Sterols and fatty acids were derivatized with pentafluorobenzoyl chloride and pentafluorobenzoyl bromide, respectively. The derivatives were assayed by ammonia negative chemical ionization GC-MS to determine the mass isotopomer distribution (MID) of the compounds (Bederman et al. 2004a, b; Kelleher and Masterson 1992; Lindenthal et al. 2002). All analyses were run with double or triple injection. Mass isotopomers are designated as M, M1, M2,..., M*i*, where *i* is the number of mass units above that of the unlabeled isotopomers M.

Results

Mass isotopomer spectral analysis of cholesterol synthesis

Until the recent demonstration of peroxisomal β-oxidation contributing to acetyl-CoA for malonyl-CoA synthesis, peroxisomal β-oxidation has not been considered as a substantial source of acetyl-CoA (Reszko et al. 2004). However, little information is available on the fate of peroxisomal acetyl-CoA. It has been shown that peroxisomal enzymes can convert acetyl-CoA (presumably derived from very long-chain fatty acid oxidation) to FPP via HMG-CoA and mevalonate (Fig. 1) (Weinhofer et al. 2006; for review see Kovacs et al. 2002). FPP leaves the peroxisome, and is converted to cholesterol in the endoplasmic reticulum (Stamellos et al. 1993). In parallel, cytosolic acetoacetyl-CoA thiolase and HMG-CoA synthase form HMG-CoA which, in the ER, is converted to mevalonate (Fig. 1). The latter diffuses or is transferred into the peroxisomes and mixes with locally made mevalonate. A related question is whether acetyl-CoA, formed by peroxisomal β-oxidation of very long-chain fatty acids is (1) directly channeled to cholesterol synthesis inside the peroxisomes, or (2) mixes with cytosolic acetyl-CoA transferred from mitochondria via citrate before being used for fatty acid and cholesterol synthesis. At least in the liver, part of the acetyl groups derived from peroxisomal oxidation can be released as free acetate (Bian et al. 2005); however, the mechanism of the transfer of peroxisomal acetyl-CoA to the cytosol needs to be further studied.

To resolve the issue of the existence of two parallel pathways leading to mevalonate and the two theories on the compartmentation of cholesterol synthesis, we used new stable isotopic techniques and data computations with ISA (Bederman et al. 2004a, b; Kelleher and Masterson 1992; Lindenthal et al. 2002). We tested whether acetyl-CoA derived from peroxisomal long-chain fatty acid oxidation (1) is directly channeled into the peroxisomal reactions linking acetyl-CoA to FPP (Pathway 1; Fig. 1), and/or (2) is partially released from the peroxisomes before it is used in the reactions forming extra-peroxisomal mevalonate (Pathway 2; Fig. 1). Experiments with (1) carbon-labeled substrates which label exclusively mitochondrial acetyl-CoA, and (2) deuterated or tritiated water which yield a measurement of total fatty acid and cholesterol synthesis, reveal an equal percent contribution of mitochondrial acetyl-CoA to fatty acid and cholesterol synthesis. Thus, tracers that label exclusively or predominantly acetyl-CoA cannot be used to test for a peroxisomal pathway of cholesterol synthesis. However, very long-chain fatty acids and medium-chain dicarboxylates undergo initial β-oxidation in peroxisomes (Mannaerts et al. 2000; Leighton et al. 1989; Bian et al. 2005), and such fatty acids, labeled on the first carbons, generate highly labeled acetyl-CoA in peroxisomes. We compared the MIDs of fatty acids and sterols in CHO-K1, peroxisome-deficient CHO (ZR-82, ZR-87), and HepG2 cells incubated with various concentrations of [1,2,3,4-$^{13}C_4$]docosanoate or [U-$^{13}C_{12}$]dodecanedioate for 24, 48, and 72 h. The MIDs of fatty acids and sterols were subjected to ISA to estimate the fractional contribution of the labeled precursor to acetyl-CoA.

The MIDs of lathosterol and cholesterol isolated from CHO-K1 cells incubated with 0.1 mM unlabeled docosanoate (C22:0) or [1,2,3,4-$^{13}C_4$]docosanoate are shown in Table 2. Lathosterol is the analyte of choice, because, unlike cholesterol, its pool is small and turns over rapidly (Lindenthal et al. 2002). It is clear, that in the presence of unlabeled docosanoate, few lathosterol molecules contained one or two ^{13}C atoms. However, in the presence of [1,2,3,4-$^{13}C_4$]docosanoate, lathosterol molecules contained up to five ^{13}C atoms, which reflects substantial labeling of acetyl-CoA used for sterol synthesis. In contrast, fatty acids (myristate, palmitate, stearate, and oleate) were not labeled from [1,2,3,4-$^{13}C_4$]docosanoate (data not shown), indicating that acetyl-CoA derived from peroxisomal β-oxidation was not released from peroxisomes and mixing with cytosolic acetyl-CoA transferred from mitochondria.

The above data obtained with [1,2,3,4-$^{13}C_4$]docosanoate were confirmed by data from experiments with [U-$^{13}C_{12}$]dodecanedioate. The latter also generates highly labeled acetyl-CoA in peroxisomes. As controls, we incubated the cells with 2 mM [1,2-$^{13}C_2$]acetate and 25 mM [U-$^{13}C_6$]glucose, which forms mitochondrial [U-$^{13}C_2$]acetyl-CoA. The labeling ratio (acetyl of sterols)/(acetyl of fatty acids) was 1.04 + 0.09 ($n = 6$) for [U-$^{13}C_6$]glucose. In contrast, in the presence of 2 mM [U-$^{13}C_{12}$]dodecanedioate for 72 h, the labeling ratio was much greater than 1 (i.e., 1.72 in CHO and 1.30 in HepG2 cells), revealing that acetyl-CoA generated by peroxisomal β-oxidation is channeled directly to sterol synthesis inside the peroxisomes. Fractional synthesis of fatty acids and sterols varied from 23 to 95%. However, the elevated sterol to fatty acid ratio for acetyl-CoA enrichment was maintained under all conditions for [U-$^{13}C_{12}$]dodecanedioate compared to [U-$^{13}C_6$]glucose. In accordance with the data from Bederman et al. (2004a) obtained in perfused rat livers, MID analysis revealed labeling of both fatty acids and sterols from the same [1,2-$^{13}C_2$]acetyl-CoA pool. Furthermore, the labeling of sterols and fatty acids was barely detectable

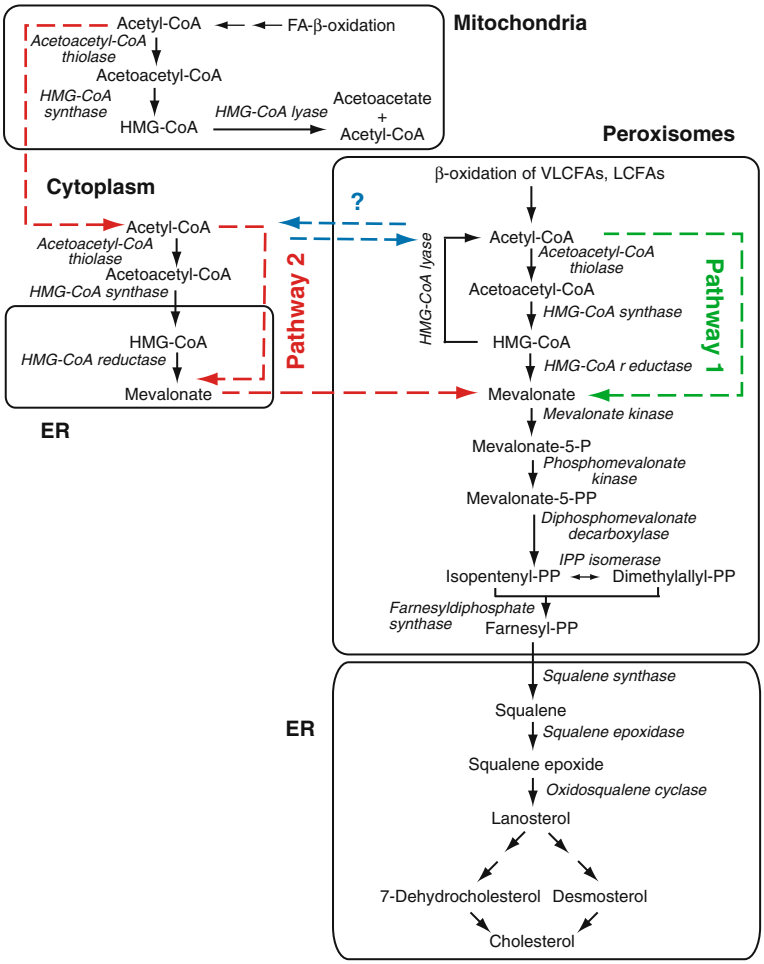

Fig. 1 Current view of the subcellular localization of cholesterol biosynthesis in mammalian cells and proposed pathways of acetyl-CoA utilization. Peroxisomal enzymes can convert acetyl-CoA, which is presumably derived from very long-chain fatty acid oxidation, to farnesyl diphosphate via HMG-CoA and mevalonate (*Pathway 1*). Reactions between mevalonate and farnesyl diphosphate are assumed to be almost exclusively peroxisomal and functional peroxisomal targeting signals have been identified in all of those enzymes. FPP leaves the peroxisomes and is converted to cholesterol in the endoplasmic reticulum (*ER*). In parallel, cytosolic acetyl-CoA is used by cytosolic acetoacetyl-CoA thiolase and HMG-CoA synthase to form HMG-CoA, which is converted to mevalonate in the ER (*Pathway 2*). The latter diffuses into the peroxisomes and mixes with locally made mevalonate. In the liver, part of the acetyl groups derived from peroxisomal oxidation are released as free acetate; however, the mechanism of the transfer of peroxisomal acetyl-CoA to the cytosol needs to be further studied. Isotopomer spectral analysis of fatty acids and sterols suggests that acetyl-CoA, formed by peroxisomal β-oxidation of very long-chain fatty acids and medium-chain dicarboxylic acids is directly channeled to cholesterol synthesis inside the peroxisomes (Pathway 1) without mixing with cytosolic acetyl-CoA transferred from mitochondria before being used for fatty acid and cholesterol synthesis (*Pathway 2*)

Table 2 Mass isotopomer distribution of sterols in CHO-K1 cells incubated with docosanoate

Sterol assayed	Substrate	Mass isotopomer distribution (mol% fractions)					
		M	M1	M2	M3	M4	M5
Cholesterol	M DOC	67.96	25.78	5.32	0.79	0.15	
	M4 DOC	62.92	25.68	7.67	2.50	1.24	
Lathosterol	M DOC	67.86	27.22	4.18	0.74		
	M4 DOC	38.78	30.11	21.71	9.39	9.64	5.46

CHO cells were cultured with either 0.1 mM unlabeled docosanoate (M DOC) or [1,2,3,4-$^{13}C_4$]docosanoate (M4 DOC) for 72 h. The mass isotopomer distribution of sterol is expressed as mol% fractions of molecule containing 0–5 ^{13}C-atoms (M–M5). The presence of M1–M4 isotopomers in the sterols from unlabeled cells reflects the natural ^{13}C-enrichment of the sterol derivatives (sterol molecule + pentafluorobenzoyl group)

(less or no more than 1%) and could not be measured with precision in the peroxisome-deficient cells ZR-82 and ZR-87. This is consistent with the disruption of the peroxisomal β-oxidation pathway due to mistargeting and degradation of peroxisomal matrix enzymes in the cytoplasm in those cells. Our data are suggestive for the localization of part of sterol synthesis in CHO and HepG2 cells in peroxisomes.

Immunofluorescence studies show that pre-squalene cholesterol biosynthetic enzymes are peroxisomal

Acetoacetyl-CoA thiolase

The formation of acetoacetyl-CoA is the first step in cholesterol and ketone body synthesis. Acetoacetyl-CoA thiolase or acetyl-CoA acetyltransferase (ACAT) activity is found in the cytosol, mitochondria, and peroxisomes of mammalian cells. Olivier et al. (2000) provided evidence for a PTS1 in mitochondrial acetoacetyl-CoA thiolase (ACAT1) and suggested that mitochondrial ACAT1 could be targeted under certain circumstances to peroxisomes via its C-terminal QKL (human) or EKL (mouse, rat).

To investigate the targeting of ACAT1, HepG2 cells were transfected with the expression vector for full-length rat ACAT1 containing a myc epitope tag between the mitochondrial and PTSs as described before (Olivier et al. 2000). Thereafter, they were processed for double immunofluorescence labeling using antibodies against the myc epitope, the peroxisomal markers AOX or peroxisomal membrane protein 70 (PMP70), as well as the mitochondrial marker cytochrome *c* (Fig. 2a–c). The full-length ACAT1 displayed a mitochondrial distribution pattern in HepG2 cells (Fig. 2a, c) that was completely superimposable over that for cytochrome *c* (data not shown). No co-localization with the punctate peroxisomal pattern for AOX (Fig. 2b, c) or PMP70 (data not shown) was observed. We also co-transfected the expression vector for full-length ACAT1 with pDsRed2-Peroxi (a mammalian expression vector that encodes a fusion of *Discosoma* sp. red fluorescent protein and the PTS1—SKL) into HepG2 cells. HepG2 cells were analyzed by direct fluorescence and immunostaining with antibodies against myc and cytochrome *c* (Fig. 2d–f). Again, the immunofluorescence pattern obtained for ACAT1 was completely superimposable over that for cytochrome *c* and did not overlap with the fluorescent punctate pattern of peroxisomes (Fig. 2f).

Our data suggest that the mitochondrial targeting sequence overrules the PTS1 and that it is unlikely that full-length mitochondrial ACAT1 is targeted to peroxisomes. Similarly, experimental evidence showed that the PTS1 signal is lower in hierarchy compared with N-terminal signals such as the mitochondrial targeting signal if they are present in the same protein (Neuberger et al. 2003b). Most probably, the binding of mitochondrial transport receptors to the N-terminus leads to an immediate mitochondrial import of the nascent polypeptide prior to binding of peroxisomal import receptors to its C-terminal PTS1. To investigate if the C-terminal tripeptide QKL might be functional as PTS1 signal, a DsRed-fusion protein containing this C-terminal peptide was expressed in HepG2 cells (Fig. 2g–i). In a functional PTS1 signal, the tripeptide SKL or conserved variants thereof would be sufficient for peroxisomal protein import in several species (Gould et al. 1990). DsRed ending in QKL, the C-terminus of human ACAT1, showed a punctate distribution (Fig. 2g) which was superimposable onto the pattern for the peroxisomal marker enzyme AOX (Fig. 2h) (for overlay, see Fig. 2i). Analysis of the carboxy-terminal 12 residues of human ACAT1 with a newly developed PTS1 prediction algorithm (Neuberger et al. 2003b) assigned human ACAT1 as probable PTS1 signal-containing protein and supported our immunofluorescence data.

Since our mass ISA data and other biochemical experiments demonstrate peroxisomal acetoacetyl-CoA formation (Thompson and Krisans 1990; Hovik et al. 1991), either the distribution of ACAT1 between peroxisomes and mitochondria is regulated by the variable usage of alternative transcription or translation initiation sites or another enzyme is involved in the acetyl-CoA condensation reaction in peroxisomes. Indeed, Antonenkov et al. (2000) purified a short chain specific thiolase from rat liver peroxisomes that is different from the thiolases involved in the breakdown of straight chain and 2-methyl-branched 3-oxoacyl-CoAs (thiolase A and B and SCPx) and that also appears to be distinct from ACAT1 and cytosolic acetoacetyl-CoA thiolase (ACAT2). Targeting to the peroxisomal matrix could also happen by "piggybacking" of a thiolase (e.g., ACAT2) with another PTS containing protein.

Dual localization of HMG-CoA reductase

To verify the subcellular localization of HMGCR in human cells, we examined the immunofluorescence pattern obtained with a monoclonal and a polyclonal HMGCR antibody. HepG2 cells were cultured in medium with lipoprotein-deficient serum (LPDS) and subsequently subjected to double-immunofluorescence labeling using antibodies against HMGCR (Fig. 3b, e)

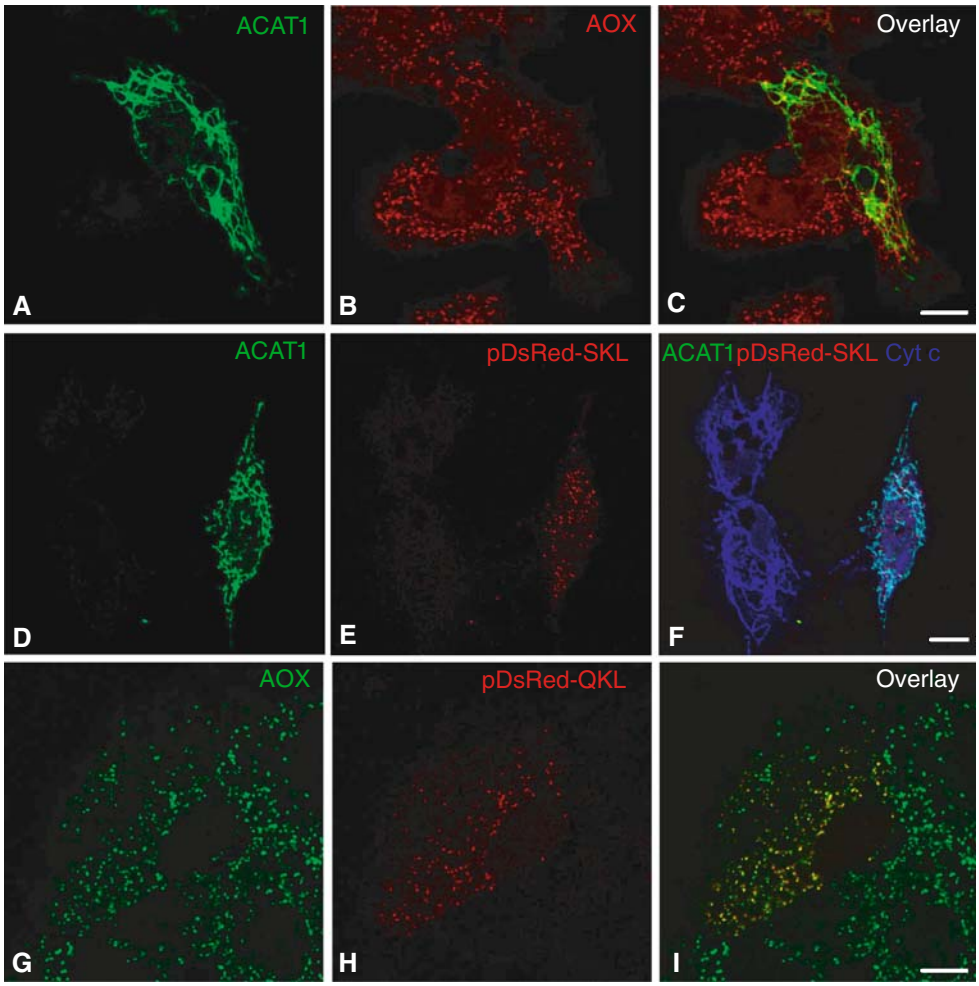

Fig. 2 The mitochondrial acetyl-CoA acetyltransferase (*ACAT1*) contains both an amino-terminal mitochondrial targeting signal and a carboxy-terminal PTS1. **a–c** HepG2 cells were transfected with full-length rat ACAT1 containing a myc epitope and processed for immunofluorescence microscopy with antibodies against myc (**a**), the peroxisomal marker acyl-CoA oxidase (*AOX*) (**b**), and the mitochondrial marker cytochrome *c*. Full-length rat ACAT1 displayed a mitochondrial distribution in HepG2 cells that was completely superimposable over that for cytochrome *c* (data not shown). Full-length ACAT1 was not found to co-localize with the punctate peroxisomal pattern for AOX (**c**). Though a few yellow punctate structures in the overlay image imply a co-localization of ACAT1 and AOX (**c**), analysis of z-sections showed that they were probably due to the proximity of some peroxisomes to the large mitochondrial structures and thus could not be resolved at the light microscopical level. **d–f** HepG2 cells were co-transfected with full-length rat ACAT1 containing a myc epitope and pDsRed2-SKL and analyzed after 48 h by direct fluorescence (**e**) and immunostaining with antibodies against myc (**d**) and cytochrome *c* (**f**). Note the co-localization of ACAT1 and cytochrome *c*, whereas ACAT1 did not co-localize with the punctate peroxisomal pattern for DsRed2-SKL (**f**). **g–i** HepG2 cells were transfected with a construct coding for DsRed2 containing the C-terminal PTS1 QKL and analyzed after 48 h by direct fluorescence (**h**) and immunostaining with an antibody against AOX (**g**). Note the co-localization of DsRed2 ending in QKL, the C-terminus of human ACAT1, and AOX in peroxisomes, demonstrating the ability of QKL to target to peroxisomes (**i**). *Bars* 10 μm

and the peroxisomal markers catalase (data not shown) or PMP70 (Fig. 3a, d). The immunofluorescence pattern obtained for HMGCR was consistent with ER labeling in all cells. However, in addition to an ER labeling pattern, a number of cells exhibited an unambiguous punctate pattern, which was directly superimposable over that for PMP70 (Fig. 3c, f) and catalase (data not shown). These results indicate that in human cells HMGCR is localized both to the ER and peroxisomes. Although probably all cells contain to some degree HMGCR in peroxisomes, peroxisomal HMGCR staining will be masked in most cells by the strong ER labeling, leading to an underestimation. Keller et al. (1986) showed that less than 5% of the total HMGCR activity is located in the peroxisomes of rat liver under control conditions compared with 20–30% of the HMGCR activity detected in peroxisomes of cholestyramine-treated animals. Since peroxisomal HMGCR seems to be encoded by the same gene as the ER enzyme (Breitling and Krisans 2002), the

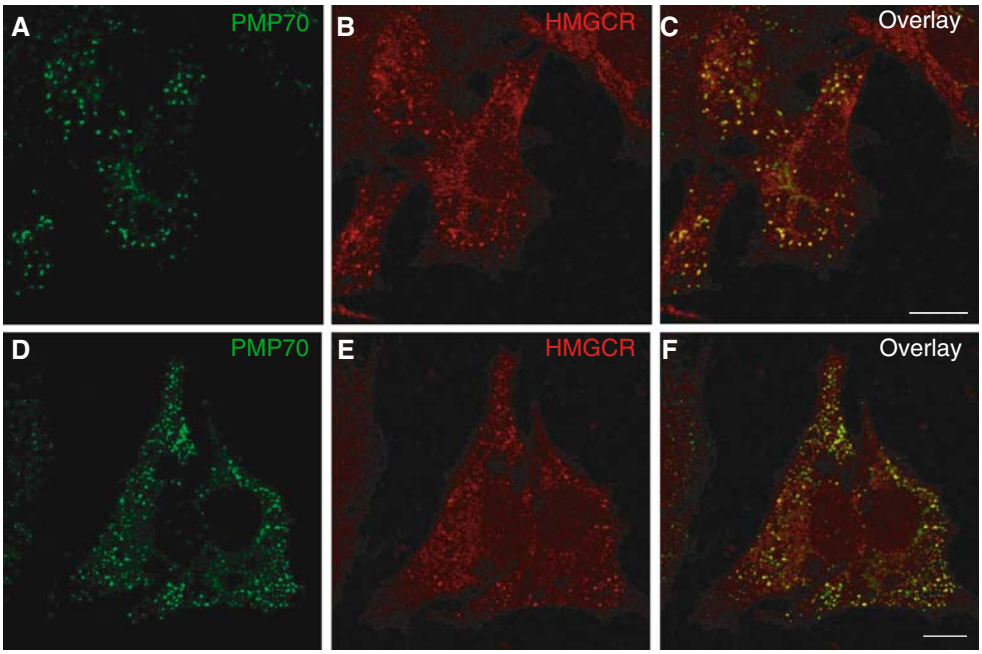

Fig. 3 Demonstration of peroxisomal localization of HMG-CoA reductase (*HMGCR*) in HepG2 cells. The cells were cultured in medium with 5% LPDS and subjected to double-immunofluorescence using anti-PMP70 followed by Alexa 488-conjugated secondary antibody (**a**, **d**) and monoclonal anti-HMGCR followed by Alexa 594-conjugated secondary antibody (**b**, **e**). Note the co-localization of PMP70 and HMG-CoA reductase in addition to the ER labeling of HMG-CoA reductase (**c**, **f**). *Bars* 10 μm

peroxisomal HMGCR activity in mammals is probably due to alternative targeting of the ER enzyme to peroxisomes by an as yet uncharacterized mechanism. Interestingly, Johnson et al. (2003) discovered a novel isoform of HMGCR by using junction microarrays to detect alternative splicing. The novel isoform was present as a mixture with the known isoform in every human tissue tested, with the exception of peripheral leukocytes in which only the novel isoform band was visible. However, the variant protein cannot catalyze the reaction of the known isoform, probably because it lacks a portion of the active site (S. Krisans and W. Kovacs, unpublished data).

Mevalonate kinase

The N-terminus of MVK contains a consensus PTS2 sequence (Table 1). This PTS2-containing region of MVK from different organisms is highly conserved (Petriv et al. 2004). We investigated the subcellular localization of MVK in HepG2 cells cultured in lipoprotein-deficient medium and in cells overexpressing rat MVK. We performed immunofluorescence microscopy with four different MVK antibodies that have been shown to be highly specific for immunoblot studies (Biardi et al. 1994). However, only the affinity-purified polyclonal antibody raised against purified MVK protein obtained from rat liver was suitable for immunofluorescence studies. We were not able to detect any immunolabeling for MVK in untransfected cells. The immunofluorescence pattern obtained with MVK antibody in HepG2 cells overexpressing MVK (Fig. 4a) is superimposable over that for catalase (Fig. 4b, for overlay see Fig. 4c). We also co-transfected the plasmid pJ3Ω-MVK (encoding rat MVK) with pDsRed2-Peroxi into HepG2 cells. Both MVK (Fig. 4d) and the red fluorescent peroxisomal protein (Fig. 4e) were co-localized in peroxisomes (see overlay Fig. 4f).

Phosphomevalonate kinase

Olivier et al. (1999) postulated a predominant peroxisomal localization of human PMVK based on expression studies in CHO cells with two green fluorescent protein (GFP) fusion proteins. One fusion protein was produced by attaching a 600 bp fragment of human PMVK cDNA, containing the putative PTS1, to the carboxyl terminus of GFP (pEGFP-PMVK). The other GFP fusion protein construct was generated similarly; however, the putative PTS1 sequence SRL was removed (pEGFP-PMVKΔPTS). We transfected HepG2 cells with the same GFP constructs to explore the localization of PMVK in human cells. Transient transfection of pEGFP-PMVK into HepG2 cells resulted in a punctate fluorescence distribution, indicative of a peroxisomal localization (Fig. 5a, d). The punctate pattern of

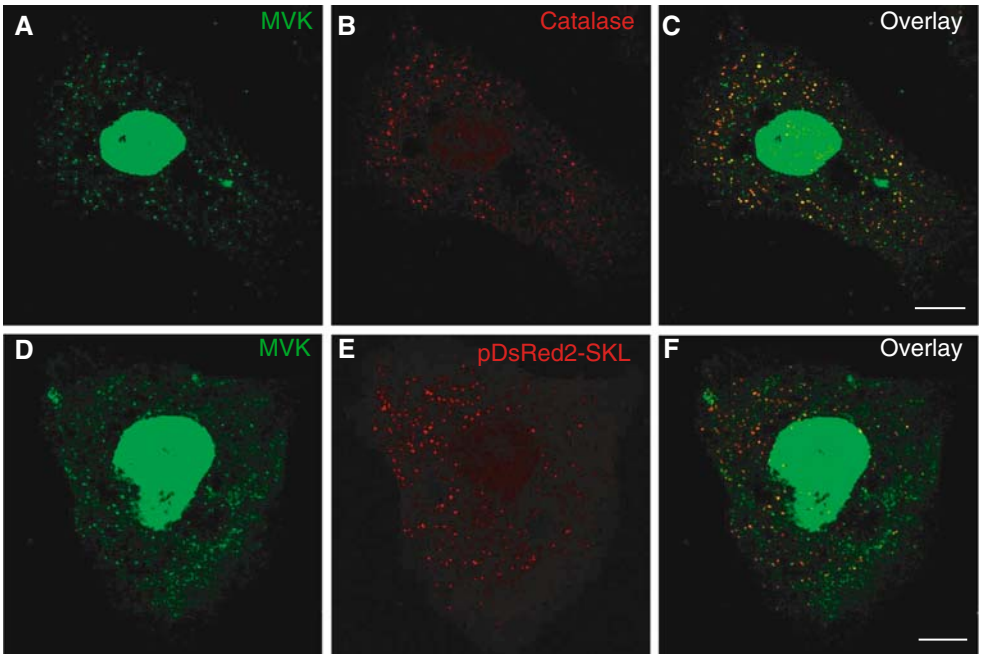

Fig. 4 Demonstration of peroxisomal localization of mevalonate kinase (*MVK*) in HepG2 cells. **a–c** The cells were transfected with pJ3Ω-MVK (encoding rat mevalonate kinase) and subjected to double-immunofluorescence labeling using affinity-purified rabbit anti-MVK followed by Alexa 488-conjugated secondary antibody (**a**) and sheep anti-human catalase followed by Texas red-conjugated secondary antibody (**b**). **d–f** HepG2 cells were co-transfected with pJ3Ω-MVK and pDsRed2-SKL and analyzed after 48 h by direct fluorescence (**e**) and immunostaining with the affinity-purified rabbit anti-MVK (**d**). Note the co-localization of mevalonate kinase with catalase (**c**) or DsRed2-SKL (**f**). Nuclear cross-reactivity of the rabbit anti-MVK was only observed in cells transfected with pJ3Ω-MVK. *Bars* 10 μm

EGFP-PMVK was superimposable over that of the peroxisomal marker enzyme catalase (Fig. 5b) and PMP70 (Fig. 5e) (see overlays Fig. 5c, f). The putative PTS1 is required for PMVK localization to the peroxisome, since cells transfected with pEGFP-PMVKΔPTS showed a diffuse, cytoplasmic fluorescence (Fig. 5g), which did not overlap with the fluorescent punctate pattern of peroxisomes obtained with antibodies against catalase (Fig. 5h, for overlay see Fig. 5i) or PMP70 (data not shown).

However, in some transfections with pEGFP-PMVK or pEGFP-PMVKΔPTS the GFP-positive cells displayed a punctate pattern (Fig. 5j) which clearly differed from the punctate fluorescence of PMP70 (Fig. 5k) or catalase (data not shown). The punctate fluorescence did not reflect a mitochondrial localization, as determined by co-localization studies using the mitochondrial marker cytochrome *c* (data not shown); a lysosomal localization, as determined by co-localization studies using the lysosome markers Limp-1 and Lamp-2 (data not shown); or endosomal localization, as determined by co-localization studies using antibodies to early endosome antigen 1 (EEA1) and Rab5 (data not shown). Interestingly, these observations are similar to those published by Hogenboom et al. (2004b), who observed a punctate pattern that did not co-localize with the punctate pattern of the peroxisomal catalase or the PMP ALDP (adrenoleukodystrophy protein). Thus, they reached the conclusion that this enzyme was not localized to peroxisomes. We assume that these GFP signals represent aggregates of misfolded protein due to overexpression, since the number of cells displaying this punctate pattern increased with high transfection efficiencies and increasing DNA amounts.

IPP isomerase

Isopentenyl diphosphate dimethylallyl diphosphate (IPP) isomerase 1 (IDI1) contains both a putative carboxy terminal PTS1 and an amino terminal PTS2 (Table 1; Paton et al. 1997). We investigated the subcellular localization of IDI1 in HepG2 cells cultured in lipoprotein-depleted medium by immunofluorescence microscopy. We performed double labeling using a highly specific affinity-purified polyclonal antibody directed against mouse IDI1 (Kovacs et al. 2004a) (Fig. 6a) and a sheep polyclonal antibody against human catalase (Fig. 6b). The immunofluorescent labeling of IDI1 showed a punctate distribution which was superimposable onto the pattern for the peroxisomal marker enzyme catalase (Fig. 6c).

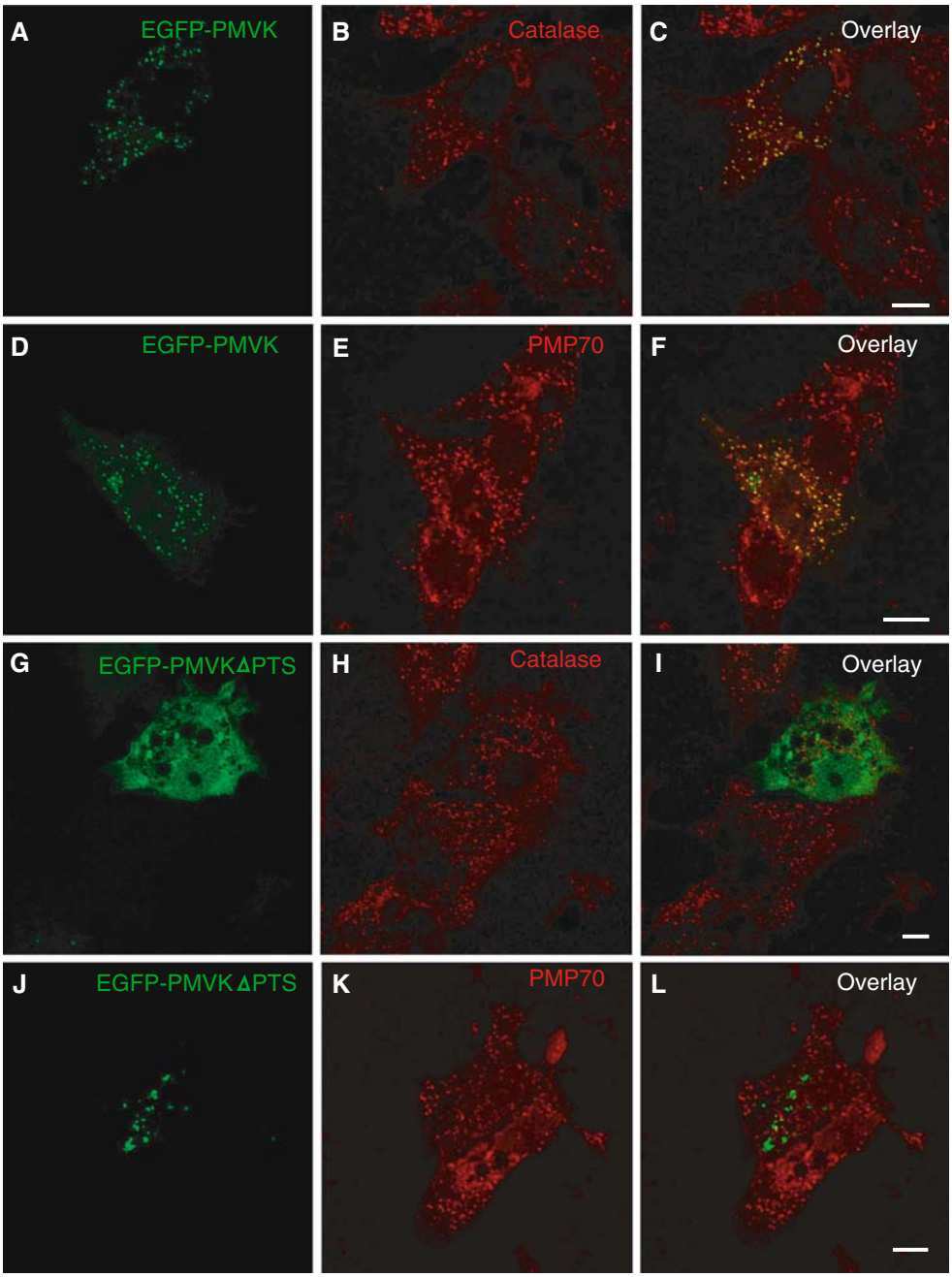

Fig. 5 Subcellular localization of human EGFP-PMVK and EGFP-PMVKΔPTS fusion proteins in HepG2 cells. **a–f** Transiently transfected pEGFP-PMVK resulted in a punctate distribution of fluorescence (**a**, **d**) which was superimposable on the immunofluorescent pattern of the peroxisomal markers catalase (**b**) and PMP70 (**e**). **g–i** Note the cytosolic green fluorescence in HepG2 cells transfected with pEGFP-PMVKΔPTS (**g**), whereas the corresponding catalase distribution remained punctate (**h**). **j–l** In some transfections with pEGFP-PMVKΔPTS or pEGFP-PMVK (data not shown) GFP-positive HepG2 cells displayed a non-organellar punctate fluorescence (**j**), which might reflect protein aggregates. Overlay images (**c**, **f**, **i**, **l**). *Bars* 10 μm

Similar to our results, obtained with the native human enzyme, expression of full-length hamster IDI1 constructs containing the PTS1 sequence HRM and an internal HA epitope tag in CHO cells, human control fibroblasts and human fibroblasts deficient in the PTS2 import pathway resulted in a superimposable punctate pattern when labeled with anti-catalase and anti-HA antibodies (Paton et al. 1997), whereas human fibroblasts deficient in the import of both PTS1 and PTS2 proteins displayed cytosolic labeling when the anti-HA antibody was used (Paton et al. 1997). Furthermore, transfection of CHO cells with HA-tagged IDI1 lacking the putative PTS1 HRM sequence revealed a cytosolic labeling with the anti-HA antibody (V. Paton,

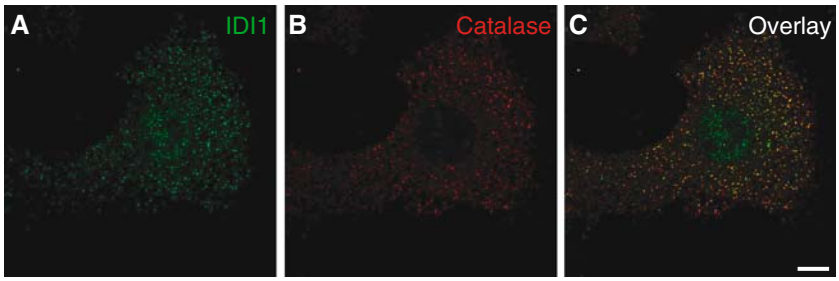

Fig. 6 Demonstration of peroxisomal localization of isopentenyl diphosphate isomerase (*IDI1*) in HepG2 cells. **a–c** HepG2 cells were incubated in medium with 5% LPDS for 24 h and subjected to double-immunofluorescence labeling using rabbit anti-IDI1 followed by Alexa 488-conjugated secondary antibody (**a**) and sheep anti-human catalase followed by Texas red-conjugated secondary antibody (**b**). The punctated immunofluorescence patterns of catalase and IDI1 are completely superimposable, indicating co-localization of the two enzymes in peroxisomes (**c**). *Bars* 10 μm

personal communication). These data showed that the PTS1 sequence is necessary for the targeting of IDI1 to peroxisomes, and that IDI1 does not use the putative PTS2 for peroxisomal targeting.

FPP synthase

Indirect immunofluorescence microscopy studies by several groups have shown that FPP synthase is localized in the peroxisomes of various cell lines (Krisans et al. 1994; Olivier et al. 2000; Gupta et al. 1999). However, subcellular fractionation studies resulted in a significant release of FPP synthase activity into the cytosolic supernatant (Krisans et al. 1994; Gupta et al. 1999). Immunofluorescence studies of myc-tagged rat FPP synthase demonstrated that FPP synthase utilizes the PTS2 import pathway and requires a PTS2-like sequence found within the amino terminal 20 amino acids for localization (Olivier et al. 2000). In this study, we investigated the subcellular localization of FPP synthase in CHO and HepG2 cells by immunofluorescence microscopy (Fig. 7). Immunofluorescence patterns for FPP synthase and catalase were similar in CHO-K1 (Fig. 7a–c), *PEX2*-transfected ZR-82 (ZR-82/pPEX2) (Fig. 7g–i), *PEX2*-transfected ZR-87 (ZR-87/pPEX2) (data not shown), and HepG2 (Fig. 7j–l) cells. These two enzymes were co-localized in peroxisomes as shown by the superimposed images (Fig. 7c, i, l). In peroxisome-deficient ZR-82 cells, the punctate pattern was no longer observed and immunofluorescence for catalase and FPP synthase was evenly distributed throughout the cytoplasm (Fig. 7d–f). A similar pattern was observed with peroxisome-deficient ZR-78 and ZR-87 cells (data not shown). Peroxisome-deficient ZR-78, ZR-82, and ZR-87 cells have mutations in *PEX2*, a gene encoding an integral PMP, resulting in nonfunctional Pex2p. Pex2p is involved in the translocation of peroxisomal matrix proteins following the docking of PTS receptors to the peroxisome membrane. When these peroxisome-deficient CHO cells were transfected with rat *PEX2* and stably selected with G418, peroxisome assembly was restored as demonstrated by the punctate fluorescence pattern obtained with antibodies to the peroxisomal matrix proteins catalase (Fig. 7h) or AOX (data not shown). Furthermore, the punctate immunofluorescence pattern for FPP synthase in *PEX2*-transfected ZR-82 (ZR-82/pPEX2) cells (Fig. 7g) coincided with that of catalase (Fig. 7h, for overlay see Fig. 7i) or AOX (data not shown), thereby demonstrating the import of FPP synthase into peroxisomes. Taken together, these results clearly show that FPP synthase is a peroxisomal protein, similar to the observations reported previously for various other cell lines.

Digitonin permeabilization studies reveal a similar intracellular distribution as immunofluorescence studies

In order to reinforce the data obtained by mass ISA of cholesterol synthesis and immunofluorescence microscopy, digitonin permeabilization of HepG2 cells and subsequent western blot analysis was used to further characterize the subcellular localization of cholesterol biosynthetic enzymes. Digitonin treatment of cells has been reported to reversibly permeabilize the plasma membrane while leaving subcellular organellar membranes intact. Digitonin permeabilizes cells by complexing with cholesterol. Since the membranes of most cell organelles contain lower levels of cholesterol than the plasma membrane, cells lose their cytoplasmic components at lower digitonin concentrations, but the organellar content remains intact. HepG2 cells were exposed to increasing concentrations of digitonin. Subsequently, the selective permeabilization and release of enzymes of cytoplasm or subcellular organelles were demonstrated with activity measurements or immunoblots of distinctive subcellular fractions. The release of

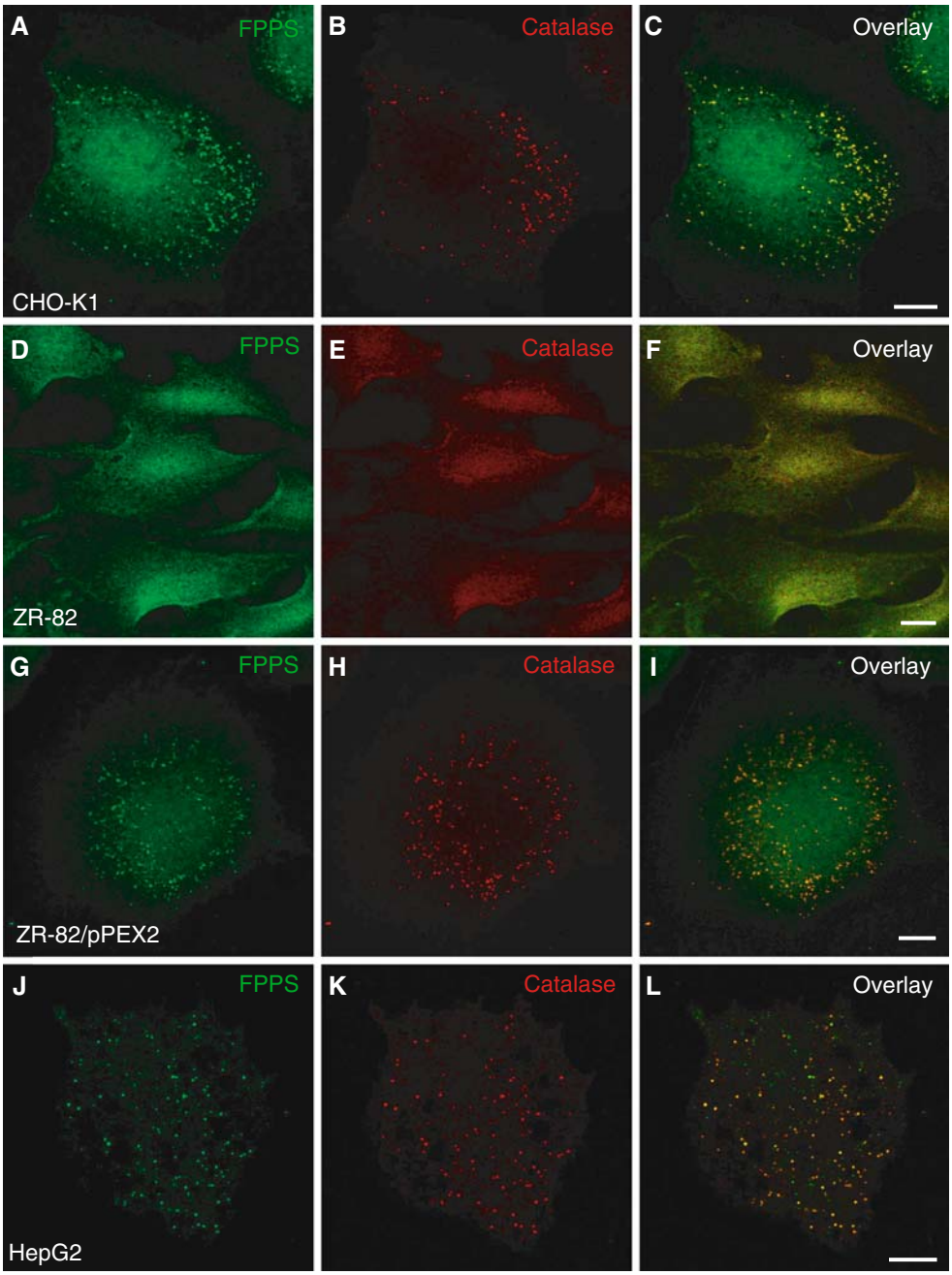

Fig. 7 Demonstration of peroxisomal co-localization of FPP synthase (*FPPS*) (**a**, **d**, **g**, **j**) and catalase (**b**, **e**, **h**, **k**) in CHO and HepG2 cells. The cells were cultured in medium with 5% LPDS for 24 h and subjected to double-immunofluorescence labeling using affinity-purified rabbit anti-rat FPP synthase followed by Alexa 488-conjugated secondary antibody and sheep anti-human catalase followed by Texas red-conjugated secondary antibody. **a–c** Wild-type CHO-KI cells. **d–f** *PEX2*-defective peroxisome-deficient CHO-K1 cells (ZR-82 cells). Note the even distribution of catalase and FPP synthase throughout the cytoplasm (**f**). **g–i** ZR-82 cells stably transformed with rat *PEX2*. Note that peroxisomes were restored and punctate structures were seen in peroxisome-deficient CHO mutants upon complementation with *PEX2* cDNA. **j–l** HepG2 cells. The punctated immunofluorescence patterns of catalase and FPP synthase are completely superimposable, indicating co-localization of the two enzymes in peroxisomes (**c**, **i**, **l**). *Bars* 10 μm

the cellular enzyme activity of phosphoglucose isomerase (PGI), a cytosolic marker, and catalase, a peroxisomal marker, were measured (Fig. 8). Most of the release of cytosolic proteins from the permeabilized cells occurred at digitonin concentrations of 50 and 150 μg/ml. Catalase remained latent (i.e., inside the peroxisomes) to a digitonin concentration of 150 μg/ml. A release of 50% of the peroxisomal matrix content,

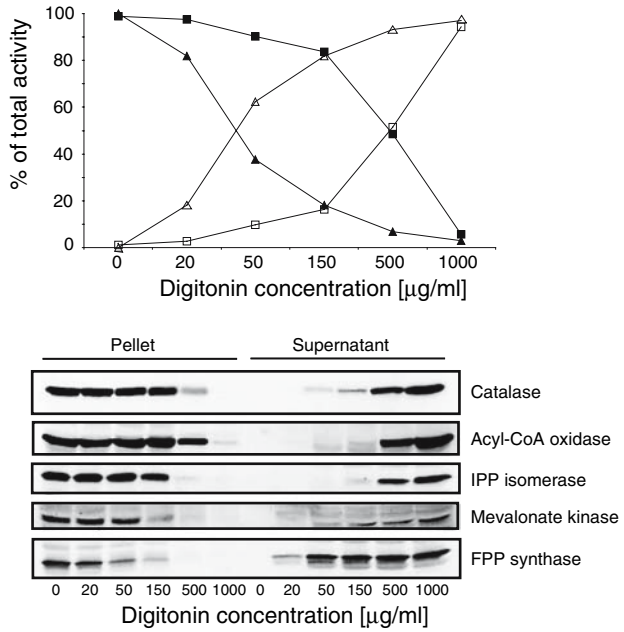

Fig. 8 Digitonin permeabilization studies in HepG2 cells. HepG2 cells were grown in lipoprotein-deficient medium for 72 h and afterwards incubated with increasing concentrations of digitonin as described in Materials and methods. Supernatant (*open symbols*) and pellet (*closed symbols*) fractions were analyzed for the activities of the cytosolic marker phosphoglucose isomerase (*triangle*) and the peroxisomal marker catalase (*square*). The patterns of distribution of the peroxisomal marker proteins catalase and AOX and the cholesterol biosynthetic enzymes IPP isomerase, mevalonate kinase and FPP synthase were determined by immunoblot analysis. Equal volumes of each fraction were analyzed. Note that the distribution pattern for IPP isomerase and mevalonate kinase was similar to the bona fide peroxisomal markers catalase and AOX, whereas FPP synthase was released on permeabilization

including catalase and AOX, into the supernatant fraction only occurred at much higher concentrations of digitonin (500–1,000 µg/ml). Immunoblot analysis of the various fractions using the antibodies against IPP isomerase (IDI1) and MVK revealed a similar distribution pattern for the IDI1 and MVK proteins as for catalase and AOX, suggestive for the localization of IDI1 and MVK to peroxisomes (Fig. 8). A significant amount of FPP synthase was released on permeabilization as demonstrated by immunoblot analysis of fractions obtained from permeabilized cells (Fig. 8). Our data are in accordance with Gupta et al. (1999), who also reported that FPP synthase is not retained after permeabilization of rat hepatoma cells with digitonin. However, former immunofluorescence studies clearly showed that FPP synthase is localized in peroxisomes (Fig. 7; Gupta et al. 1999). These data show that peroxisomal cholesterol biosynthetic enzymes display markedly different association with this organelle.

Discussion

Protein subcellular localization is a key functional characteristic of proteins. The spatial and temporal regulation of biochemical reactions in eukaryotic cells is achieved by a high degree of compartmentation. This structural differentiation facilitates interactions and yet allows the segregation of different biochemical networks. The cholesterol/isoprenoid biosynthetic pathway has been the subject of extensive studies in the previous decades due to the panoply of functions of cholesterol, its metabolites, and its immediate biosynthetic precursors in the proper functioning of cells and organisms and understanding of cholesterol homeostasis and its fine regulation is utterly essential. There is conclusive evidence for the peroxisomal localization of the pre-squalene segment of the cholesterol biosynthetic pathway in rodents (for review, see Kovacs et al. 2002). However, the role of peroxisomes in cholesterol biosynthesis in humans has been questioned in recent reports by Waterham and coworkers (Hogenboom et al. 2004a, b, c). To resolve the conflicting reports concerning the localization of enzymes of cholesterol synthesis, we used immunofluorescence microscopy, selective permeabilization techniques, and new stable isotope labeling techniques and data computations with ISA.

Our present findings obtained by immunofluorescence and selective digitonin permeabilization experiments clearly show that the pre-squalene segment of the cholesterol biosynthetic pathway is localized to peroxisomes, which contradicts the results from Hogenboom et al (2004a, b, c). We obtained further proof for the localization of the pre-squalene segment of cholesterol synthesis in peroxisomes by MID analysis of fatty acids and sterols in HepG2 and CHO cells, since acetyl-CoA derived from peroxisomal β-oxidation of very long-chain fatty acids and medium-chain dicarboxylic acids was preferentially channeled to cholesterol synthesis inside the peroxisomes. In contrast, fatty acids were not labeled from [1,2,3,4-$^{13}C_4$]docosanoate or [U-$^{13}C_{12}$]dodecanedioate, indicating that acetyl-CoA derived from peroxisomal β-oxidation was not released from peroxisomes and mixing with the cytosolic acetyl-CoA transferred from mitochondria before being used for fatty acid and cholesterol synthesis.

In addition, further proof of the peroxisomal localization of cholesterol biosynthetic enzymes comes from studies by Aboushadi et al. (2000) and Weinhofer et al. (2006). These studies have demonstrated that HMGCR localized to peroxisomes is more resistant to inhibition by statins, a class of cholesterol-lowering drugs, than ER HMGCR. Weinhofer et al. (2006)

showed that lovastatin suppresses cholesterol biosynthesis from [1-^{14}C]acetate and [1-^{14}C]C8:0, but not from [1-^{14}C]C24:0 as precursor, indicating that [1-^{14}C]acetyl-CoA units generated by peroxisomal β-oxidation do not leave peroxisomes but rather are used for cholesterol synthesis.

Furthermore, recent studies by Antonenkov et al. (2004a, b) indicate that the mammalian peroxisomal membrane allows free access into the particles only to small, water-soluble metabolites, while restricting penetration of more bulky organic molecules, such as cofactors (NAD/H, NADP/H, CoA) and phosphorylated substrates. The permeability properties of the peroxisomal membrane require that the export and import of redox equivalents into and out of peroxisomes, and also the transport of acyl-/acetyl-groups across the membrane occur via shuttle systems. Peroxisomes may possess a separate pool of cofactors that is functionally independent from the corresponding pool of cofactors in the surrounding cytoplasm. Since phosphorylated products of mevalonate are not able to cross freely the peroxisomal membrane, it is likely that the multi-stage conversion of mevalonate to FPP will take place in one compartment. The export of FPP across the peroxisomal membrane would be expected to require peroxisomal membrane transport as has been shown for other compounds (AMP and ATP) bearing negatively charged phosphate groups (Palmieri et al. 2001). Such a peroxisomal transport system for FPP has not been identified yet.

Limitations of the subcellular fractionation approach may contribute to the discrepancy met with subcellular localization studies of cholesterol biosynthetic enzymes. The fragility of peroxisomes under in vitro conditions is well known and the uncertainty surrounding the quality of isolated peroxisomes diminishes the validity of in vitro experiments. Some soluble peroxisomal matrix proteins are known to easily leak from peroxisomes during the isolation of peroxisomes (Alexson et al. 1985; Antonenkov et al. 2004a, b). Several peroxisomal oxidases (urate oxidase, L-α-hydroxyacid oxidase and D-amino acid oxidase) also possess no latency in digitonin-permeabilized rat hepatocytes, although this type of treatment is much more protective for peroxisomes than tissue homogenization and fractionation (Verleur and Wanders 1993). This is also exemplified by a study from Yoshihara et al. (2001), which clearly showed by immunolocalization studies that the NADP-linked isocitrate dehydrogenase 1 (IDH1) is a predominantly, if not exclusively, peroxisomal enzyme in rat hepatocytes, whereas subcellular fractionation studies revealed that the enzyme is predominantly cytosolic and only partially peroxisomal.

It should be noted, that the conflicting data that have been published recently on the peroxisomal involvement in the biosynthesis of cholesterol are based on immunolocalization studies using antisera against MVK, PMVK, and MPD (Hogenboom et al. 2004a, b, c). It must be pointed out that not all antibodies will work equally well in all assays. Cell staining techniques place exceptional demands on antibody specificity in order to bind specifically to antigens in the presence of high concentrations of other macromolecules. Antibody preparations that are satisfactory for techniques such as immunoblotting may show spurious cross-reactions in cell staining. For example, we performed cell-staining experiments with four different polyclonal antibodies against MVK that have been shown to be highly specific for immunoblot studies (Biardi et al. 1994); however, only one was suitable for immunofluorescence studies. Furthermore, significant protein levels of cholesterol biosynthetic enzymes in cells and tissues are only present if the cholesterol biosynthetic pathway is induced due to low cholesterol levels or inhibition by statins. For example, while MVK was clearly detected in the matrix of peroxisomes in the liver from cholestyramine plus mevinolin-treated rats, a treatment that upregulates the cholesterol biosynthetic pathway, no immunolabeling was detected in the livers from control animals (Biardi et al. 1994). Therefore, great care should be taken with the interpretation of results obtained with immunolocalization studies of cholesterol biosynthetic enzymes on human liver sections.

Recently, several computational methods have been developed with the aim of predicting subcellular and peroxisomal localization of proteins (Emanuelsson et al. 2003; Neuberger et al. 2003a, b; Guda and Subramaniam 2005; Xie et al. 2005). The assumption is that conservation of function and localization is correlated and thus a prediction of a protein being peroxisomal is strengthened if also its orthologs in other organisms are predicted to be peroxisomal. Thus, if localization to mammalian peroxisomes has been shown in some species, orthologs in other organisms are also assumed to be peroxisomal. For lack of data on PTS2 proteins, in silico prediction methods focus on proteins carrying the C-terminal PTS1. The isoprenoid biosynthesis pathway contains three enzymes with PTS1 motifs (Table 1). PMVK and IDI1 were predicted to be peroxisomal in several organisms using the methods described by Emanuelsson et al. (2003), Neuberger et al. (2003a, b), Xie et al. (2005), and Guda and Subramaniam (2005), and their peroxisomal localization was confirmed in our study. Furthermore, we also showed that the C-terminal tripeptide QKL of human

ACAT1 is a functional PTS1 signal. One of the limitations of the computational methods is its inability to accurately predict proteins localized in multiple locations (e.g., HMGCR, acetoacetyl-CoA thiolase in the cholesterol biosynthetic pathway). However, several peroxisomal proteins that have multiple subcellular localizations have been identified, including alanine-glyoxylate aminotransferase (Oatey et al. 1996; Oda et al. 2000; Huber et al. 2005), malonyl-CoA decarboxylase (Sacksteder et al. 1999), and α-methylacyl-CoA racemase (Kotti et al. 2000; Amery et al. 2000).

In summary, our results clearly show that the first part of cholesterol synthesis from acetyl-CoA to FPP occurs in peroxisomes and refute the hypothesis that peroxisomes are not involved in the biosynthesis of isoprenoids and cholesterol. Furthermore, the importance of peroxisomes for the maintenance of cholesterol homeostasis in vivo has clearly been demonstrated in the peroxisome-deficient *PEX2* knockout mouse model (Kovacs et al. 2004a). We are at present in the process of a more extensive investigation into the role of acetyl-CoA generated in peroxisomes for fatty acid and sterol synthesis. Since it is difficult to reconcile the different data regarding the localization of cholesterol biosynthetic enzymes using subcellular fractionation and immunohistochemical techniques, the mass isotopomer distribution analysis in combination with mathematical modeling provides a powerful method for metabolic pathway analysis.

Acknowledgments This work was supported by National Institutes of Health (NIH) grants DK58238 and DK58040 to S.K.K. We thank Drs. Eveline Baumgart-Vogt and Herbert Stangl for helpful discussions and comments on the manuscript.

References

Aboushadi N, Shackelford JE, Jessani N, Gentile A, Krisans SK (2000) Characterization of peroxisomal 3-hydroxy-3-methylglutaryl coenzyme A reductase in UT2 cells: sterol biosynthesis, phosphorylation, degradation, and statin inhibition. Biochemistry 39:237–247

Aden DP, Fogel A, Plotkin S, Damjanov I, Knowles BB (1979) Controlled synthesis of HBsAG in a differentiated human liver carcinoma-derived cell line. Nature 282:615–616

Alexson SEH, Fujiky Y, Shio H, Lazarow PB (1985) Partial disassembly of peroxisomes. J Cell Biol 101:294–305

Amery L, Fransen M, De Nys K, Mannaerts GP, Veldhoven PP van (2000) Mitochondrial and peroxisomal targeting of 2-methylacyl-CoA racemase in humans. J Lipid Res 41:1752–1759

Antonenkov VD, Croes K, Waelkens E, Veldhoven PP van, Mannaerts GP (2000) Identification, purification and characterization of an acetoacetyl-CoA thiolase from rat liver peroxisomes. Eur J Biochem 267:2981–2990

Antonenkov VD, Sormunen RT, Hiltunen JK (2004a) The rat liver peroxisomal membrane forms a permeability barrier for cofactors but not for small metabolites in vitro. J Cell Sci 117:5633–5642

Antonenkov VD, Sormunen RT, Hiltunen JK (2004b) The behavior of peroxisomes in vitro: mammalian peroxisomes are osmotically sensitive particles. Am J Physiol Cell Physiol 287:C1623–C1635

Bederman IR, Reszko AE, Kasumov T, David F, Wasserman DH, Kelleher JK, Brunengraber H (2004a) Zonation of labeling of lipogenic acetyl-CoA across the liver: implications for studies of lipogenesis by mass isotopomer analysis. J Biol Chem 279:43207–43216

Bederman IR, Kasumov T, Reszko AE, David F, Brunengraber H, Kelleher JK (2004b) In vitro modeling of fatty acid synthesis under conditions simulating the zonation of lipogenic [^{13}C]acetyl-CoA enrichment in the liver. J Biol Chem 279:43217–43226

Beier K, Völkl A, Hashimoto T, Fahimi HD (1988) Selective induction of peroxisomal enzymes by the hypolipidemic drug bezafibrate. Detection of modulations by automatic image analysis in conjunction with immunoelectron microscopy and immunoblotting. Eur J Cell Biol 46:383–393

Bian F, Kasumov T, Thomas KR, Jobbins KA, David F, Minkler PE, Hoppel CL, Brunengraber H (2005) Peroxisomal and mitochondrial oxidation of fatty acids in the heart, assessed from the 13C labeling of malonyl-CoA and the acetyl moiety of citrate. J Biol Chem 280:9265–9271

Biardi L, Krisans SK (1996) Compartmentalization of cholesterol biosynthesis. J Biol Chem 271:1784–1788

Biardi L, Sreedhar A, Zokaei A, Vartak NB, Bozeat RL, Shackelford JE, Keller GA, Krisans SK (1994) Mevalonate kinase is predominantly localized in peroxisomes and is defective in patients with peroxisome deficiency disorders. J Biol Chem 269:1197–1205

Breitling R, Krisans SK (2002) A second gene for peroxisomal HMG-CoA reductase? A genomic reassessment. J Lipid Res 43:2031–2036

Chambliss KL, Slaughter CA, Schreiner R, Hoffmann GF, Gibson KM (1996) Molecular cloning of human phosphomevalonate kinase and identification of a consensus peroxisomal targeting sequence. J Biol Chem 271:17330–17334

Dammai V, Subramani S (2001) The human peroxisomal targeting signal receptor, Pex5p, is translocated into the peroxisomal matrix and recycled to the cytosol. Cell 105:187–196

Emanuelsson O, Elofsson A, Heijne G von, Cristóbal S (2003) *In silico* prediction of the peroxisomal proteome in fungi, plants and animals. J Mol Biol 330:443–456

Ghys K, Fransen M, Mannaerts GP, Veldhoven PP van (2002) Functional studies on human Pex7p: subcellular localization and interaction with proteins containing a peroxisome-targeting signal type 2 and other peroxins. Biochem J 365:41–50

Goldstein JL, Brown MS (1990) Regulation of the mevalonate pathway. Nature 343:425–430

Gould SJ, Keller GA, Schneider M, Howell SH, Garrard LJ, Goodman JM, Distel B, Tabak H, Subramani S (1990) Peroxisomal protein import is conserved between yeast, plants, insects and mammals. EMBO J 9:85–90

Guda C, Subramaniam S (2005) TARGET: a new method for predicting protein subcellular localization in eukaryotes. Bioinformatics 21:3963–3969

Gupta SD, Mehan RS, Tansey TR, Chen HT, Goping G, Goldberg I, Shechter I (1999) Differential binding of proteins to peroxisomes in rat hepatoma cells: unique association of enzymes involved in isoprenoid metabolism. J Lipid Res 40:1572–1584

Hogenboom S, Tuyp JJM, Espeel M, Koster J, Wanders RJA, Waterham HR (2004a) Mevalonate kinase is a cytosolic enzyme in humans. J Cell Sci 117:631–639

Hogenboom S, Tuyp JJM, Espeel M, Koster J, Wanders RJA, Waterham HR (2004b) Phosphomevalonate kinase is a cytosolic protein in humans. J Lipid Res 45:697–705

Hogenboom S, Tuyp JJM, Espeel M, Koster J, Wanders RJA, Waterham HR (2004c) Human mevalonate pyrophosphate decarboxylase is localized in the cytosol. Mol Genet Metab 81:216–224

Hovik R, Brodal B, Bartlett K, Osmundsen H (1991) Metabolism of acetyl-CoA by isolated peroxisomal fractions: formation of acetate and acetoacetyl-CoA. J Lipid Res 32:993–999

Huber PAJ, Birdsey GM, Lumb MJ, Prowse DTR, Perkins TJ, Knight DR, Danpure CJ (2005) Peroxisomal import of human alanine:glyoxylate aminotransferase requires ancillary targeting information remote from its C terminus. J Biol Chem 280:27111–27120

Johnson JM, Castle J, Garrett-Engele P, Kan Z, Loerch PM, Armour CD, Santos R, Schadt EE, Stoughton R, Shoemaker DD (2003) Genome-wide survey of human alternative pre-mRNA splicing with exon junction microarrays. Science 302:2141–2144

Kelleher JK, Masterson TM (1992) Model equations for condensation biosynthesis using stable isotopes and radioisotopes. Am J Physiol 262:E118–E125

Keller GA, Barton MC, Shapiro DJ, Singer SJ (1985) 3-hydroxy-3-methylglutaryl-coenzyme A reductase is present in peroxisomes in normal rat liver cells. Proc Natl Acad Sci USA 82:770–774

Keller GA, Pazirandeh M, Krisans SK (1986) 3-Hydroxy-3-methylglutaryl coenzyme A reductase localization in rat liver peroxisomes and microsomes of control and cholestyramine-treated animals: quantitative biochemical and immunoelectron microscopical analyses. J Cell Biol 103:875–886

Kotti TJ, Savolainen K, Helander HM, Yagi A, Novikov DK, Kalkkinen N, Conzelmann E, Hiltunen JK, Schmitz W (2000) In mouse alpha-methylacyl-CoA racemase, the same gene product is simultaneously located in mitochondria and peroxisomes. J Biol Chem 275:20887–20895

Kovacs WJ, Faust PL, Keller GA, Krisans SK (2001) Purification of brain peroxisomes and localization of 3-hydroxy-3-methylglutaryl coenzyme A reductase. Eur J Biochem 268:4850–4859

Kovacs WJ, Olivier LM, Krisans SK (2002) Central role of peroxisomes in isoprenoid biosynthesis. Prog Lipid Res 41:369–391

Kovacs WJ, Shackelford JE, Tape KN, Richards MJ, Faust PL, Fliesler SJ, Krisans SK (2004a) Disturbed cholesterol homeostasis in a peroxisome-deficient PEX2 knockout mouse model. Mol Cell Biol 24:1–13

Kovacs WJ, Schrader M, Walter I, Stangl H (2004b) The hypolipidemic compound cetaben induces changes in Golgi morphology and vesicle movement. Histochem Cell Biol 122:95–109

Krisans SK, Ericsson J, Edwards PA, Keller GA (1994) Farnesyldiphosphate synthase is localized in peroxisomes. J Biol Chem 269:14165–14169

Lametschwandtner G, Brocard C, Fransen M, Veldhoven P van, Berger J, Hartig A (1998) The difference in recognition of terminal tripeptides as peroxisomal targeting signal 1 between yeast and human is due to different affinities of their receptor Pex5p to the cognate signal and to residues adjacent to it. J Biol Chem 273:33635–33643

Leighton F, Bergseth S, Rortveit T, Christiansen EN, Bremer J (1989) Free acetate production by rat hepatocytes during peroxisomal fatty acid and dicarboxylic acid oxidation. J Biol Chem 264:10347–10350

Lindenthal B, Aldaghlas TA, Holleran AL, Sudhop T, Berthold HK, Bergmann K von, Kelleher JK (2002) Isotopomer spectral analysis of intermediates of cholesterol synthesis in human subjects and hepatic cells. Am J Physiol Endocrinol Metab 282:E1222–E1230

Lüers G, Hashimoto T, Fahimi HD, Völkl A (1993) Biogenesis of peroxisomes: isolation and characterization of two distinct peroxisomal populations from normal and regenerating rat liver. J Cell Biol 121:1271–1280

Mannaerts GP, Veldhoven PP van, Casteels M (2000) Peroxisomal lipid degradation via beta- and alpha-oxidation in mammals. Cell Biochem Biophys 32:73–87

Mukai S, Ghaedi K, Fujiki Y (2002) Intracellular localization, function, and dysfunction of the peroxisome-targeting signal type 2 receptor, Pex7p, in mammalian cells. J Biol Chem 277:9548–9561

Neuberger G, Maurer-Stroh S, Eisenhaber B, Hartig A, Eisenhaber F (2003a) Motif refinement of the peroxisomal targeting signal 1 and evaluation of taxon-specific differences. J Mol Biol 328:567–579

Neuberger G, Maurer-Stroh S, Eisenhaber B, Hartig A, Eisenhaber F (2003b) Prediction of peroxisomal targeting signal 1 containing proteins from amino acid sequence. J Mol Biol 328:581–592

Oatey PB, Lumb MJ, Danpure CJ (1996) Molecular basis of the variable mitochondrial and peroxisomal localization of alanine-glyoxylate aminotransferase. Eur J Biochem 241:374–385

Oda T, Mizuno T, Ito K, Funai T, Ichiyama A, Miura S (2000) Peroxisomal and mitochondrial targeting of serine:pyruvate/alanine:glyoxylate aminotransferase in rat liver. Cell Biochem Biophys 32:277–281

Olivier LM, Chambliss KL, Gibson KM, Krisans SK (1999) Characterization of phosphomevalonate kinase: chromosomal localization, regulation, and subcellular targeting. J Lipid Res 40:672–679

Olivier LM, Kovacs W, Masuda K, Keller GA, Krisans SK (2000) Identification of peroxisomal targeting signals in cholesterol biosynthetic enzymes: AA-CoA thiolase, HMG-CoA synthase, MPPD, and FPP synthase. J Lipid Res 41:1921–1935

Palmieri L, Rottensteiner H, Girzalsky W, Scarcia P, Palmieri F, Erdmann R (2001) Identification and functional reconstitution of the yeast peroxisomal adenine nucleotide transporter. EMBO J 20:5049–5059

Paton VG, Shackelford JE, Krisans SK (1997) Cloning and subcellular localization of hamster and rat isopentenyl diphosphate dimethylallyl diphosphate isomerase. J Biol Chem 272:18945–18950

Petriv OI, Tang L, Titorenko VI, Rachubinski RA (2004) A new definition for the consensus sequence of the peroxisome targeting signal type 2. J Mol Biol 341:119–134

Rachubinski RA, Subramani S (1995) How proteins penetrate peroxisomes. Cell 83:525–528

Reszko AE, Kasumov T, David F, Jobbins KA, Thomas KR, Hoppel CL, Brunengraber H, Rosiers C des (2004) Peroxisomal fatty acid oxidation is a substantial source of the acetyl moiety of malonyl-CoA in rat heart. J Biol Chem 279:19574–19579

Sacksteder KA, Morrell JC, Wanders RJA, Matalon R, Gould SJ (1999) *MCD* encodes peroxisomal and cytoplasmic forms of malonyl-CoA decarboxylase and is mutated in malonyl-CoA decarboxylase deficiency. J Biol Chem 274:24461–24468

Schrader M, Fahimi HD (2004) Mammalian peroxisomes and reactive oxygen species. Histochem Cell Biol 122:383–393

Stamellos KD, Shackelford JE, Tanaka RD, Krisans SK (1992) Mevalonate kinase is localized in rat liver peroxisomes. J Biol Chem 267:5560–5568

Stamellos KD, Shackelford JE, Shechter I, Jiang G, Conrad D, Keller GA, Krisans SK (1993) Subcellular localization of squalene synthase in rat hepatic cells. Biochemical and immunochemical evidence. J Biol Chem 268:12825–12836

Subramani S (1993) Protein import into peroxisomes and biogenesis of the organelle. Annu Rev Cell Biol 9:445–478

Thompson SL, Krisans SK (1990) Rat liver peroxisomes catalyze the initial step in cholesterol synthesis. The condensation of acetyl-CoA units into acetoacetyl-CoA. J Biol Chem 265:5731–5735

Verleur N, Wanders RJA (1993) Permeability properties of peroxisomes in digitonin-permeabilized rat hepatocytes. Eur J Biochem 218:75–82

Wanders RJ (2004) Metabolic and molecular basis of peroxisomal disorders: a review. Am J Med Genet 126A:355–375

Weinhofer I, Kunze M, Stangl H, Porter FD, Berger J (2006) Peroxisomal cholesterol biosynthesis and Smith–Lemli–Opitz syndrome. Biochem Biophys Res Commun 345:205–209

Xie D, Li A, Wang M, Fan Z, Feng H (2005) LOCSVMPSI: a web server for subcellular localization of eukaryotic proteins using SVM and profile of PSI-BLAST. Nucleic Acids Res 33:W105–W110

Yoshihara T, Hamamoto T, Munakata R, Tajiri R, Ohsumi M, Yokota S (2001) Localization of cytosolic NADP-dependent isocitrate dehydrogenase in the peroxisomes of rat liver cells: biochemical and immunocytochemical studies. J Histochem Cytochem 49:1123–1131

Zhang Y, Agarwal KC, Beylot M, Soloviev MV, David F, Reider MW, Anderson VE, Tserng KY, Brunengraber H (1994) Nonhomogeneous labeling of liver extra-mitochondrial acetyl-CoA. Implications for the probing of lipogenic acetyl-CoA via drug acetylation and for the production of acetate by the liver. J Biol Chem 269:11025–11029